

# Structural And Photoluminescent Studies Of SrAl<sub>2</sub>O<sub>4</sub>: Dy<sup>3+</sup>, Ce<sup>3+</sup> Phosphors

Riya Neema<sup>1,a)</sup>, M. Saleem<sup>2,b)</sup>, P. K. Sharma<sup>1</sup>, M. Mittal<sup>1</sup>

<sup>1</sup>Govt. Autonomous Holkar Science College, Department of Physics, Indore 452001, India

<sup>2</sup>School of Physics, VigyanBhawan, Devi Ahilya University, Khandwa, Road Campus, Indore 452001, India

<sup>a)</sup>rianeema@gmail.com

<sup>b)</sup>mscphy7@gmail.com

**Abstract:** Hereby, we report the structural and photoluminescent properties of Sr<sub>1-x</sub>Dy<sub>x-z</sub>Ce<sub>z</sub>Al<sub>2</sub>O<sub>4</sub> [ $x = 0.03, 0.02, 0.01$  and  $z = 0.01, 0.02$  and  $0.03$  respectively] phosphors. The sample synthesis was successfully carried out by solid state reaction route. The crystal structure and the type of phase formed was witnessed by X-ray diffraction characterization where the spectra analysis revealed that the as synthesized samples have crystallized into the monoclinic phase with the assigned space group of P21/n. The samples were observed to have the presence of additional phase corresponding to SrCO<sub>3</sub>. The XRD results were further confirmed through the Fourier Transform Infra-Red (FTIR) characterization technique where fingerprint absorption peaks confirm the XRD results. Photoluminescent studies revealed the highly intense broad glow curve corresponding to the Ce<sup>3+</sup> presence in SrAl<sub>2</sub>O<sub>4</sub> matrix around 390 nm whereas the weak and broad glow curves corresponding to the Dy<sup>3+</sup> are observed in the higher region of visible range of electromagnetic spectrum.

**Keywords:** Phosphors, Structure, Photoluminescence, FTIR.

## INTRODUCTION

Luminescent materials i.e. phosphors, emit light after absorption of energy from an excitation source. These phosphors can be classified on the basis of their chemical family, application or by the excitation source. When we classify them on the excitation basis, they are categorized as photoluminescent (PL), cathodoluminescent, X-ray luminescent, triboluminescent, sonoluminescent, electroluminescent, thermoluminescent, chemiluminescent and bioluminescent.

PL materials are energy-storing materials as they absorb the visible light from the source, store the energy, and later on release the energy as visible light giving rise to the persistent afterglow in the dark [1]. This character glorifies a wide application of these materials in the fields like the dial plates of glow watch, warning signs, automobile, ship and other instruments, escape routes, and textiles, etc. [2]. Strontium aluminate phosphors have attracted much attention as phosphors when activated by europium and dysprosium as they display excellent luminescent properties [3]. Aluminates have several valuable properties such as high radiation intensity, color purity, longer afterglow, chemical stability, harmlessness and no hazardous radiation, etc [1-4].

Strontium aluminate, SrAl<sub>2</sub>O<sub>4</sub> host, exhibits tridymite type structure, even though the crystal structure is related to AB<sub>2</sub>O<sub>4</sub> spinel structure explained due to the large size of Sr<sup>2+</sup> (1.18 Å), avoiding the spinel structure formation. The structure consist of tetrahedral [AlO<sub>4</sub>]<sup>5-</sup> layers that share vertex forming six-member rings. Strontium cations, Sr<sup>2+</sup>, are found within the hexagonal cavities formed by AlO<sub>4</sub> tetrahedra. Sr<sup>2+</sup> cations can occupy two non-equivalent sites (with nine adjacent oxygen ions) with coordination 7 or 7+2 [5, 6]

In the present study, we have replaced Eu<sup>3+</sup> by Ce<sup>3+</sup> dopant in the SrAl<sub>2</sub>O<sub>4</sub> with varied concentrations. The samples are prepared by conventional solid state reaction route. The report is focused on the structural and luminescent studies and the influence of the dopants with their varying concentration.

## EXPERIMENTAL DETAILS

The highly crystalline phosphors of the type  $\text{Sr}_{1-x}\text{Dy}_{x-z}\text{Ce}_z\text{Al}_2\text{O}_4$  [ $x=0.03, 0.02, 0.01$  and  $z = 0.01, 0.02$  and  $0.03$  respectively] were synthesized by solid state reaction route in which the starting materials used were  $\text{SrCO}_3, \text{Al}_2\text{O}_3, \text{Dy}_2\text{O}_3, \text{Eu}_2\text{O}_3, \text{CeO}_2$ . The starting materials were weighed as per the requirement indicated by the calculations. The stoichiometric ratio of the above weighed oxides were mixed in the agate-mortar with intense grinding for 5h. The powder was then calcined at  $1000^\circ\text{C}$  for 10h. The calcined powder was re-grinded and re-calcined but this time at  $1200^\circ\text{C}$  to remove the impurities and to obtain the crystalline sample. Lastly, the powder was ground again for an hour to get the fine powder before going for characterization.

Structural and phase formation of  $\text{Sr}_{1-x}\text{Dy}_{x-z}\text{Ce}_z\text{Al}_2\text{O}_4$  [ $x=0.03, 0.02, 0.01$  and  $z = 0.01, 0.02$  and  $0.03$  respectively] phosphors was investigated via X-ray diffraction technique employing using Bruker D8 Advance X-ray diffractometer with  $\text{CuK}\alpha_1$  ( $1.5406\text{\AA}$ ) radiation over the angular range of  $10^\circ < 2\theta < 80^\circ$  with step size of  $0.02$ . Fourier Transformation Infrared Spectroscopy (FTIR) was done by Perkin Elmer FT-IR/FIR spectroscopy in the range of  $400$  to  $4000\text{ cm}^{-1}$ . Photoluminescence measurements were carried out using Edinburgh Instrument FLS920-s fluorescence spectrometer. All the characterizations were carried out at room temperature.

## RESULTS AND DISCUSSIONS

The phosphors of  $\text{Dy}^{3+}$  and  $\text{Ce}^{3+}$  doped  $\text{SrAl}_2\text{O}_4$  were synthesized via solid state method. The structural and phase formation was confirmed via the most reliable one XRD characterization. The spectra of the synthesized samples was recorded in the angular range of  $10^\circ - 80^\circ$ . The data was plotted and has been depicted in the Figure 1. The analysis revealed that the prepared sample is not a single phase in nature but reveals the presence of two phases. The phase in addition to the  $\text{SrAl}_2\text{O}_4:\text{Ce}^{3+}, \text{Dy}^{3+}$  was found to be the  $\text{SrCO}_3$  represented by # tag. The desired aluminate phase has crystallized into the monoclinic (P21/n) phase [7]. The lattice parameters were calculated for  $\text{SrAl}_2\text{O}_4:\text{Ce}^{3+}, \text{Dy}^{3+}$  where  $a = 8.447\text{\AA}$ ,  $b = 8.818\text{\AA}$  and  $c = 5.163\text{\AA}$ . The spectra on observation reveals the formation of highly crystalline samples, the intensity and sharpness of the main peak is the witness. Further, the width of the characteristic peak indicates larger average particle size of the samples prepared which on calculation using classical Scherer formula, t

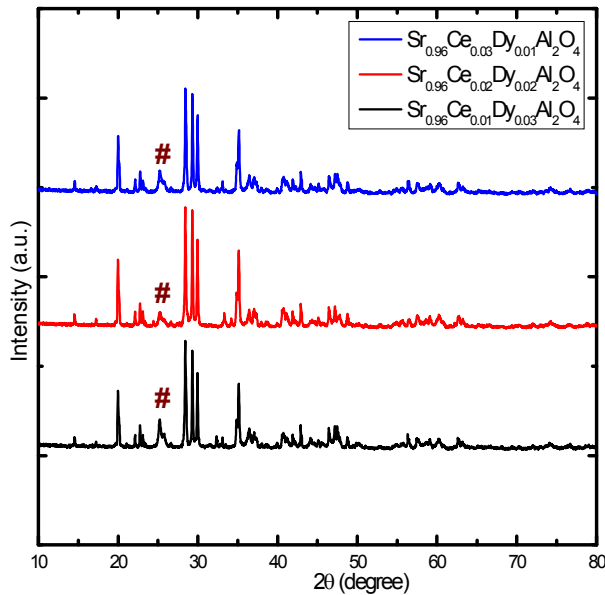


**FIGURE 1.** XRD spectra of  $\text{Sr}_{1-x}\text{Dy}_{x-z}\text{Ce}_z\text{Al}_2\text{O}_4$  [ $x=0.03, 0.02, 0.01$  and  $z = 0.01, 0.02$  and  $0.03$  resp.] phosphors

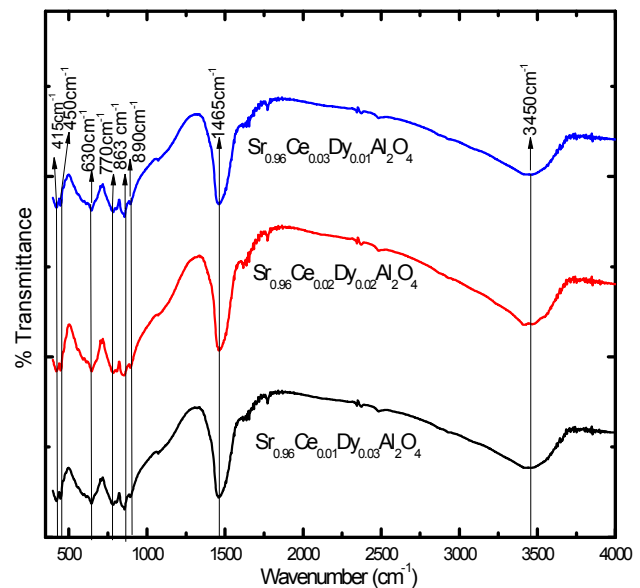


**FIGURE 2.** FTIR spectra of  $\text{Sr}_{1-x}\text{Dy}_{x-z}\text{Ce}_z\text{Al}_2\text{O}_4$  [ $x=0.03, 0.02, 0.01$  and  $z = 0.01, 0.02$  and  $0.03$ ]

$= k\lambda/\square \cos\theta$ , [where ‘k’ is called shape factor and  $k= 0.9$ ,  $\lambda = 0.546 \text{ \AA}$ , is the wavelength used,  $\theta$  is the Bragg’ angle and  $\square$  is the full width at half maximum] were found to be 57nm, 68 nm and 61nm for  $\text{Sr}_{1-x}\text{Dy}_{x-z}\text{Ce}_z\text{Al}_2\text{O}_4$  [ $x = 0.03, 0.02, 0.01$  and  $z = 0.01, 0.02$  and  $0.03$  respectively]. The XRD spectrum also reveals that  $\text{Ce}^{3+}$  and  $\text{Dy}^{3+}$  doping has not changed the desired aluminate’s structure which is attributed to the uniform dispersion of the dopants at Sr site. This characteristic is assigned to nearly the same ionic radii of the  $\text{Sr}^{2+}$  (1.12  $\text{\AA}$ ) and that of dopants  $\text{Ce}^{3+}$  (1.034  $\text{\AA}$ ) and  $\text{Dy}^{3+}$  (0.908  $\text{\AA}$ ) [8,9].

FTIR technique is considered to be a fast and the accurate spectroscopic measurement to determine the quality material components. Mostly, the measurement is carried out from  $4000 \text{ cm}^{-1}$  to  $400 \text{ cm}^{-1}$  i.e. a middle Infra-red region. The spectra of the as prepared phosphors has been displayed in the Figure2. The important region in the displayed spectra of the synthesized samples of the aluminate phosphor is the fingerprint region ranging from  $400 \text{ cm}^{-1}$  to  $1500 \text{ cm}^{-1}$ . The bands below  $1000 \text{ cm}^{-1}$  are typically inherent active IR vibration modes of the strontium aluminate. The absorption bands observed at  $415 \text{ cm}^{-1}$  and  $450 \text{ cm}^{-1}$  are assigned to the symmetric bending of O-Al-O bond. The absorption bands at  $630 \text{ cm}^{-1}$ ,  $770 \text{ cm}^{-1}$ ,  $863 \text{ cm}^{-1}$ ,  $890 \text{ cm}^{-1}$  are anti-symmetric stretching bands of Sr-O vibrations in  $\text{SrAl}_2\text{O}_4$ . The sharp absorption peak appearing at  $1465 \text{ cm}^{-1}$  has not been reported in the literature though it exists there and hence the origin of the said peak is still a mystery [10]. The peak at  $3450 \text{ cm}^{-1}$  can be assigned to the -OH group present due to the highly hygroscopic nature of the rare earths used in the synthesized phosphor [11, 12].

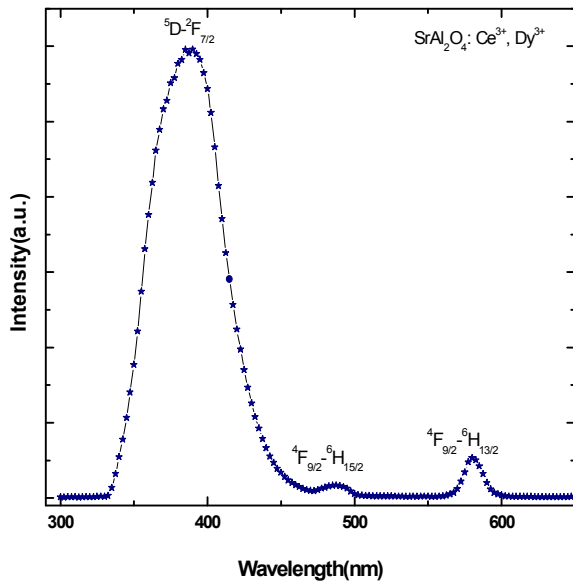


FIGURE 3. PL spectrum of  $\text{Sr}_{0.96}\text{Dy}_{0.03}\text{Ce}_{0.01}\text{Al}_2\text{O}_4$  phosphor

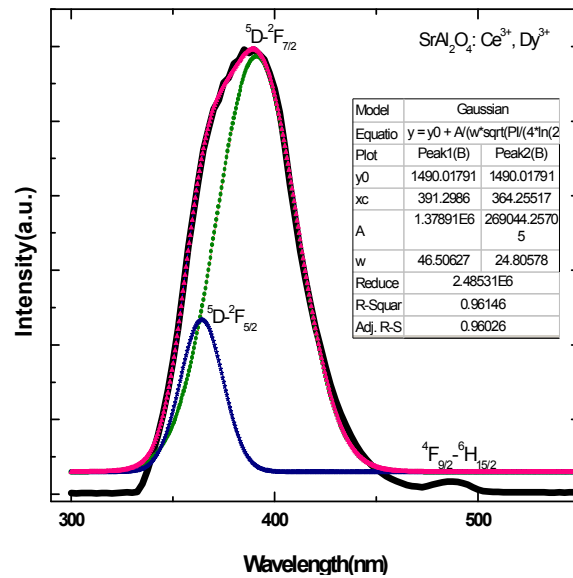


FIGURE 4. Convolved PL spectrum of  $\text{Sr}_{0.96}\text{Dy}_{0.03}\text{Ce}_{0.01}\text{Al}_2\text{O}_4$  phosphor.

The photoluminescence emission spectra of  $\text{Sr}_{0.96}\text{Dy}_{0.03}\text{Ce}_{0.01}\text{Al}_2\text{O}_4$  phosphor are presented in Figure 3 under the excitation in UV region (325nm). The emission of as prepared phosphor is observed to be intense and broad emission peak located about 390nm predominantly due to the 5d-4f transition of  $\text{Ce}^{3+}$  ion which can be fitted by two Gaussian peaks display in Figure 4. The fitted peaks are located at around 364 and 391 nm.  $\text{Ce}^{3+}$  has only one outer electron and only two spin-orbital splitting 4f states ( $^2F_{7/2, 5/2}$ ) [13], hence the excited state energy structure of  $\text{Ce}^{3+}$  is simpler than other trivalent rare-earth ions. The emission spectrum of  $\text{Ce}^{3+}$  should be composed of double bands in view of the transition from  $5d \rightarrow ^2F_{7/2}$  and  $^2F_{5/2}$  states which are separated by crystal field splitting [14]. The theoretical energy difference of splitting between  $^2F_{7/2}$  and  $^2F_{5/2}$  of  $\text{Ce}^{3+}$  is about  $2000 \text{ cm}^{-1}$ . However the energy difference between 364nm and 391nm is about  $1900 \text{ cm}^{-1}$ , which is in good agreement to the experimentally observed and theoretically estimated values. The co-dopant  $\text{Dy}^{3+}$  is one of the important rare earth ions which play a major role in the production of different types of light emitting materials. The luminescence spectrum of  $\text{Dy}^{3+}$  consists of two intense bands in the visible spectral range at around 487nm (blue) and 580nm (yellow), they are assigned to the  $\text{Dy}^{3+}$  electronic transition of  $^4F_{9/2} \rightarrow ^6H_{15/2}$  and  $^4F_{9/2} \rightarrow ^6H_{13/2}$ . energy levels respectively reported

elsewhere[15]. However, in the present case, the peaks are shifted towards the higher wavelength side which is collective effect of the presence of the  $Ce^{3+}$  ion in the matrix of  $SrAl_2O_4$ .

In conclusion, the solid state products of  $Sr_{1-x}Dy_xCe_zAl_2O_4$  [ $x = 0.03, 0.02, 0.01$  and  $z = 0.01, 0.02$  and  $0.03$  respectively] phosphors were found to have crystalized into the monoclinic phase where an additional phase of  $SrCO_3$  is also present. The phase formation of the as prepared samples were further verified via FTIR characterization where the fingerprint absorption peaks displayed witnesses the XRD results. The PL glow curve for  $Sr_{0.96}Dy_{0.03}Ce_{0.01}Al_2O_4$  displays an intense broad glow peak around 390nm which is actually double due to the  $Ce^{3+}$  ion in the matrix of  $SrAl_2O_4$ . In addition the low intense glow curves observed at higher wavelengths are attribute to the presence of  $Dy^{3+}$  ion.

## ACKNOWLEDGEMENTS

UGC-DAE-CSR, Indore (M.P.), as an institute is acknowledged for providing characterization facilities. Authors are grateful to Dr. V. Ganeshan, centre director, Dr. M. Gupta for XRD facility. Dr. Geeta Sarasar, Department of Chemistry, Holkar Science College is acknowledged for FTIR characterization. Authors express gratitude to Dr. Kinny Pandey, IIT Indore (M.P.) for PL characterization.

## REFERENCES

1. C. Chang, D. Mao, J. Shen, C. Feng, J. Alloys Comp. **348** 224 (2003).
2. T. Katsumata, T. Nabaie, K. Sasajima, S. Kumuro, T. Morikawa, J. Electrochem. Soc. **144** 243(1997).
3. W. Jia, H. Yuan, L. Lu, et al., J. Cryst. Growth, **200** 179 (1999).
4. C. N. Xu, in Encyclopedia of Smart Materials, edited by M. Schwartz Wiley, New York, **1** 190 (2002).
5. G. Groppi, C. Cristiani, P. Forzatti, J. Mater. Sci. **29** (1994) and H. Matsui, C. N. Xu, and H. Tateyama, Appl. Phys. Lett. **78** 1236(2001).
6. M. Somani, M. Saleem, AIP Conference Proceedings **1953** 030212 (2018) and M. Saleem, D. Varshney, AIP Conference Proceedings **1953** 030093(2018).
7. M. Saleem, A. Mishra and D. Varshney, J Supercond Nov Magn, **31** 943 (2018) and M. Saleem, D. Singh, A. Mishra and D. Varshney, Mater. Res. Express **6** 026304 (2019).
8. M. Saleem and D. Varshney, J. Alloys. Compd. **708** 309(2017) and M. Saleem, D. Varshney, RSC Adv., **8** 1600(2018).
9. H. Zhang, H. Yamada, N. Terasaki, C. N. Xua, Appl. Phys. Lett., **91** 081905 (2007).
10. K. Nakamoto, Infrared and Raman spectra of Organic and coordination compounds, (Wiley, New York, 1986)
11. M. Ayvacikli, A. Ege, N. Can, Opt. Mater. **34** 138 (2011).
12. I.P.Sahu, D.P.Bisen, N. Brahme, R.K. Tamrakar, R. Shrivastava, J Mater. Sci: Mater. Electron. **26** 8824 (2015).
13. Y. Gong, X. Xu, W. Zeng, C. Wu, Y. Wang, Physics Procedia, **29** 86 (2012).
14. J. Zhang, L.H. Huang, L.X. Yang, Z.D. Lu, X.Y. Wang, G.L. Xu, E.P. Zhang, H.B. Wang, Z. Kong, J.H. Xi, and Z.G. Ji, J. Alloys Compd. **676** 37 (2016).
15. N. Lakshminarasimhan, U.V. Varadaraju, Mater. Res. Bull. **43** 2946 (2008).